

Center for Advanced Materials

# CAM

Submitted to Journal of the  
American Ceramic Society

## Densification and Shear Deformation in $\text{YBa}_2\text{Cu}_3\text{O}_{6+\delta}$ Powder Compacts

M.N. Rahaman, L.C. De Jonghe, and M-Y. Chu

January 1988

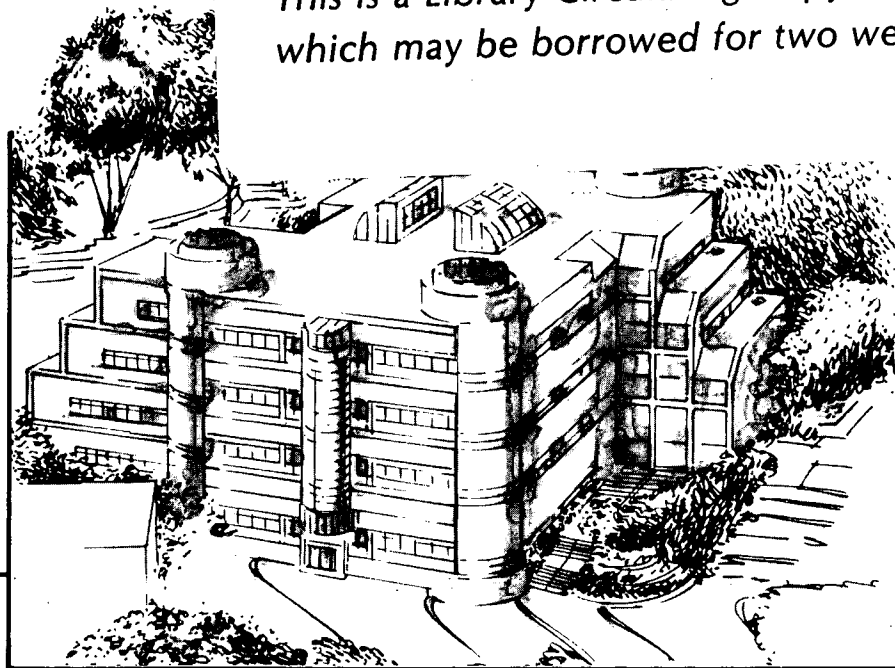
RECEIVED  
LAWRENCE  
BERKELEY LABORATORY

APR 19 1988

LIBRARY AND  
DOCUMENTS SECTION

### TWO-WEEK LOAN COPY

*This is a Library Circulating Copy  
which may be borrowed for two weeks.*



**Materials and Chemical Sciences Division**  
**Lawrence Berkeley Laboratory • University of California**  
ONE CYCLOTRON ROAD, BERKELEY, CA 94720 • (415) 486-4755

LBL-24764  
c.2

## **DISCLAIMER**

This document was prepared as an account of work sponsored by the United States Government. While this document is believed to contain correct information, neither the United States Government nor any agency thereof, nor the Regents of the University of California, nor any of their employees, makes any warranty, express or implied, or assumes any legal responsibility for the accuracy, completeness, or usefulness of any information, apparatus, product, or process disclosed, or represents that its use would not infringe privately owned rights. Reference herein to any specific commercial product, process, or service by its trade name, trademark, manufacturer, or otherwise, does not necessarily constitute or imply its endorsement, recommendation, or favoring by the United States Government or any agency thereof, or the Regents of the University of California. The views and opinions of authors expressed herein do not necessarily state or reflect those of the United States Government or any agency thereof or the Regents of the University of California.

DENSIFICATION AND SHEAR DEFORMATION IN  $\text{YBa}_2\text{Cu}_3\text{O}_{6+\delta}$  POWDER  
COMPACTS

Mohamed N. Rahaman  
Ceramic Engineering Department  
University of Missouri-Rolla  
Rolla, MO 65401

Lutgard C. De Jonghe\* and May-Ying Chu\*  
Center For Advanced Materials  
Lawrence Berkeley Laboratory  
and Department of Material Science and Mineral Engineering  
University of California, Berkeley, CA 94720

ABSTRACT

Powder compacts having a nominal composition of  $\text{YBa}_2\text{Cu}_3\text{O}_{6+\delta}$  were sintered in air at temperatures between 910 and 940°C in a loading dilatometer that permitted the application of small, controlled uniaxial stresses to the sintering compact. The highest density of 95% of the theoretical was obtained after sintering without load for  $\approx 2$  hours at 935°C. The application of constant, small uniaxial stresses produced extensive shear deformation and a small increase in the densification rate. The measured ratio of the densification rate to the creep rate provided strong support for the presence of a liquid phase during sintering. The data allowed the measurement of the ratio of the creep viscosity to the densification viscosity, which was  $\approx 0.8$  over the density range 0.6-0.8, and the sintering stress, which was  $\approx 400\text{kPa}$ . These data show that extensive shear deformation and significant increases in the densification rates may be achieved by the application of relatively small uniaxial stresses ( $\approx 1\text{ MPa}$ ) during sintering of  $\text{YBa}_2\text{Cu}_3\text{O}_{6+\delta}$  powder compacts.

1. INTRODUCTION

---

\*Member, the American Ceramic Society

The discovery by Bednorz and Muller<sup>1</sup> of superconductivity above 30K in the La-Ba-Cu-O system, and the more recent discovery of superconductivity above 90K in the Y-Ba-Cu-O system by Chu and coworkers<sup>2,3</sup>, and later by others<sup>4-6</sup>, have been reviewed briefly by Clarke<sup>7</sup>. The superconductivity in the Y-Ba-Cu-O system was attributed to an yttrium barium cuprate phase,  $\text{YBa}_2\text{Cu}_3\text{O}_{6+\delta}$ , with a crystal structure based on a distorted oxygen-deficient perovskite.<sup>8-11</sup>

Initially, fabrication of the high temperature superconducting oxides appeared to be carried out with minimal control of the densification process and the microstructural parameters, and difficulties were reported in achieving densities over 90% of the theoretical one. The control of microstructure, and particularly grain size, grain boundary porosity and pore network morphology are important factors in optimizing the current carrying capabilities and the ease of conversion to the orthorhombic phase. In some applications, eg. when high mechanical strength is needed, near-theoretical densities may be required, while in others, the ease of rapid conversion to the orthorhombic phase may require as high a density as is possible while maintaining a fully connected pore network. The present study is intended to clarify some of the parameters that affect densification and the mechanisms that are likely to be involved in the densification process.

This paper reports on an investigation into the sintering of powder compacts with a nominal composition of  $\text{YBa}_2\text{Cu}_3\text{O}_{6+\delta}$ . The superconducting properties of the sintered samples, and others sintered under different conditions will be the subject of a

subsequent report. The powders were prepared by solid state reaction, and the sintering experiments were carried out in air at temperatures between 910 and 940°C in a loading dilatometer. The technique of loading dilatometry,<sup>12,13</sup> which combines densification measurements with simultaneous, low-load uniaxial creep measurements, has been shown to assist in clarifying some aspects of the sintering process in a number of materials.<sup>14-17</sup> It would be of interest to apply the technique to the sintering of  $\text{YBa}_2\text{Cu}_3\text{O}_{6+\delta}$ .

## 2. EXPERIMENTAL PROCEDURE

Powders of the ceramic superconducting compound with a nominal composition of  $\text{YBa}_2\text{Cu}_3\text{O}_{6+\delta}$  ( $\delta$  undetermined) were prepared by solid state reaction between  $\text{Y}_2\text{O}_3^*$ ,  $\text{CuO}^+$ , and  $\text{BaCO}_3^\#$ , at 850°C, for 24 hours. These powders were milled while dispersed in anhydrous toluene in a polyethylene container using high purity zirconia balls<sup>\*\*</sup> as a milling medium. The calcination at 850°C produced a very friable powder that was easily ground with a mortar and pestle. X-ray examination of the calcined powder showed it to be single phase  $\text{YBa}_2\text{Cu}_3\text{O}_{6+\delta}$  to within the detection limit ( $\approx 1\%$ ). The resulting powder ( $\approx 1 \mu\text{m}$  average particle size) was dried and stored in a vacuum desiccator prior to use. Small cylindrical compacts (6mm in diameter by 5mm) with a relative density of  $\approx 0.50 \pm 0.01$  were prepared by uniaxial pressing in a die at  $\approx 20 \text{ MPa}$ .

For the sintering studies, the samples were held in the

---

\*  $\text{Y}_2\text{O}_3$ : purity 99.999% +, Sigma Chemical Co., St. Louis, MO 63178.  
 $\text{CuO}$ : purity 99.999% +, Aldrich Chemical Co., Milwaukee, WI 53231.  
 $\text{BaCO}_3$ : purity 99.999%, Noah Chemical Co., Farmingdale NY 11735.

\*\* Toya Soda, USA, Inc., 1700 Water Place, Suite 204, Atlanta, GA 30339.

dilatometer and then introduced rapidly into the dilatometer furnace which was kept at 800°C. After reaching thermal equilibrium ( $\approx 10$  min) the sample was heated at a constant rate of 5°C per min to the isothermal sintering temperature. To study the effect of temperature on densification rate, experiments were performed between 910 and 940°C under no applied load.

For the creep-sintering experiments, conducted at 915°C, constant loads of 0.2 and 0.4 N, corresponding initially to stresses of 70 and 140 kPa, were applied to the sintering compact. The temperature of 915°C was chosen so that densification was almost completed within 2 h. For these experiments the load was applied immediately after the isothermal sintering temperature was reached, at which time the density of the sample had increased to 55% of the theoretical. After sintering the densities of the samples were verified using Archimedes' principle.

In a separate set of experiments, creep-sintering was terminated after times between 0 and 2 h, and the dimensions of these compacts were measured using a micrometer. Fracture surfaces, and polished and etched surfaces were examined by scanning electron microscopy. A solution of 40% HF was used as the etchant. The average grain sizes of four separate specimens were measured from polished and etched surfaces of samples sintered for 5, 20, 60 and 120 min.

### 3. DATA ANALYSIS

The experimental measurements provided data for the change in

length and radius of the sample with time. The data were converted to true strains by using the definitions appropriate for large deformation. If  $L(t)$  and  $R(t)$  are the time-dependent length and radius, respectively, of the sample, then the axial strain rate,  $\dot{\epsilon}_z$ , and the radial strain rate,  $\dot{\epsilon}_r$ , may be written as

$$\dot{\epsilon}_z = d[\ln (L/L_0)]/dt \quad (1)$$

$$\dot{\epsilon}_r = d[\ln (R/R_0)]/dt \quad (2)$$

where  $L_0$  and  $R_0$  are the initial length and radius, respectively. The creep strain rate,  $\dot{\epsilon}_c$ , and the volumetric densification rate,  $\dot{\epsilon}_\rho$  can then be calculated from the relations<sup>18</sup>

$$\dot{\epsilon}_c = (2/3)(\dot{\epsilon}_z - \dot{\epsilon}_r) \quad (3)$$

$$\dot{\epsilon}_\rho = \dot{\rho}/3\rho = -(\dot{\epsilon}_z + 2\dot{\epsilon}_r) \quad (4)$$

where  $\rho$  is the relative density. If the externally applied uniaxial stress on the sintering compact is  $\sigma_z$ , then the mean hydrostatic stress experienced by the compact is

$$\sigma_h = \Sigma/\phi = \sigma_z/3 \quad (5)$$

where  $\Sigma/\phi$  is the sintering stress due to reduction in surface area, and  $\phi$  is a porosity-dependent term<sup>19-21</sup> called the stress intensification factor. According to Eq. (5), the term  $\Sigma/\phi$  has the same effect on densification as an externally applied compressive hydrostatic stress of the same magnitude.

During the experiment, the cross-sectional area of the sample

changed with time and is given  $A = \pi R^2$ . Using Eq. (2), then

$$A = A_0 \exp(2\epsilon_r) \quad (6)$$

where  $A_0$  is the initial cross-sectional area of the sample given by  $A_0 = \pi R_0^2$ . The total load on the sample consisted of a constant load,  $P$ , (0.2 and 0.4 N), applied by an electromagnetic loading device, and a small load,  $S$ , due to the dilatometer spring that is required to maintain contact between the push rod and the sample. The spring load,  $S$ , was measured as described earlier<sup>16</sup>, and was found to decrease approximately linearly from  $\approx 0.01$  N to zero during shrinkage of the sample. The uniaxial stress on the sample is then given by

$$\sigma_z = (P + S) / [A_0 \exp(2\epsilon_r)] \quad (7)$$

#### 4. RESULTS

The effects of temperature and low uniaxial stresses on the sintering of  $\text{YBa}_2\text{Cu}_3\text{O}_{6+\delta}$  powder compacts are described separately in the following sections.

##### (1) Effect of Temperature

Figure 1 shows the axial strain,  $\epsilon_z$ , vs time for samples sintered in air at temperatures between 915 and 935°C under no applied load. At any time, the shrinkage increases significantly within this temperature range. At the end of the experiment (2 h) the radial strain,  $\epsilon_r$ , was slightly less than the axial strain, i.e.  $\epsilon_{rf} \approx 0.95\epsilon_{zf}$ , and this was believed to be due to



the effect of the dilatometer spring load.

The relative density,  $\rho$ , shown in Fig. 2, was calculated from the shrinkage kinetics using Eq. (4), and by assuming that the same proportionality constant existed between  $\epsilon_z$  and  $\epsilon_r$  throughout the course of an experiment. A value of  $6.35 \text{ Mgm}^{-3}$  was taken as the theoretical density of the single-phase  $\text{YBa}_2\text{Cu}_3\text{O}_{6+\delta}$  compound. The final densities calculated from the initial density and the shape changes were within 2% of the values obtained using Archimedes' method. At any value of  $\rho$ , the densification rate increases rapidly with temperature and, in the temperature range used, the densification has almost stopped after  $\approx 2$  h. The final density increases with the sintering temperatures shown, but above  $\approx 935^\circ\text{C}$  there is almost no further increase. Below  $\approx 910^\circ\text{C}$  densification is relatively slow. A temperature range of  $920 - 940^\circ\text{C}$  is therefore appropriate for sintering these samples to high densities in air.

The final densities of 0.87 to 0.95 obtained at the different sintering temperatures in this work compare quite favorably with those obtained by Cima and Rhine<sup>22</sup> and by Chu and Dunn<sup>23</sup> using more elaborate processing techniques, and are higher than those reported by others<sup>24,25</sup> using more conventional powder processing techniques.

## (2) Effect of Low Applied Stress

The experiments to investigate the effect of low applied uniaxial stress on the sintering of  $\text{YBa}_2\text{Cu}_3\text{O}_{6+\delta}$  powder compacts were carried out in air at  $915^\circ\text{C}$ . Figure 3 shows the results for the axial strain,  $\epsilon_z$ , vs time for the samples sintered under

initial stress of 0, 70, and 140 kPa. Each curve is the average of two experiments under the same conditions, and  $t = 0$  represents the attainment of the isothermal sintering temperature. The applied stresses cause a significant increase in  $\epsilon_z$  at any time. The extent of this increase is much larger than those seen in similar experiments on pure, single-phase, polycrystalline oxides<sup>14,15</sup> but is comparable to those observed for materials that sinter by viscous flow<sup>16</sup> and liquid-phase<sup>17</sup> mechanisms. In Fig. 4, the data for  $\epsilon_z$  are plotted vs the radial strain,  $\epsilon_r$  for the uniaxial stresses used. The intersection of the data at  $\epsilon_z \approx \epsilon_r \approx 0.03$  represents the time at which the isothermal sintering temperature was reached, when the stresses were applied rapidly.

The data of Figs. 3 and 4 were used to calculate the creep strain,  $\epsilon_c$ , and the relative density,  $\rho$ , according to Eqs. (3) and (4), and the results are shown in Figs. 5 and 6. The applied stresses cause extensive creep but only a small increase in the density, as observed earlier for other ceramic powders.<sup>14-17</sup> In Fig. 5 the small creep strain (<1%) observed for the sample sintered under "zero" load, i.e.  $P = 0$  in Eq. (7), may be due to the small spring load,  $S$ , of the dilatometer. The final densities of the samples sintered under applied stresses of 0 and 140 kPa are 0.87 and 0.90, respectively. The data for the density of the sample sintered under a stress of 70 kPa have been omitted from Fig. 6 to preserve clarity.

The creep strain rate,  $\dot{\epsilon}_c$ , and the volumetric densification rate,  $\dot{\epsilon}_\rho$ , were calculated from Figs. 5 and 6 by fitting smooth curves to the data and differentiating. As in previous work<sup>14,16</sup> the data for  $\dot{\epsilon}_c$  had to be corrected for the increase in the applied stress due to the changing cross-sectional area during

sintering (eq. (7)). The  $\dot{\epsilon}_c$  values were evaluated at a constant stress based on the initial area of the compact and by making use of the observation that  $\dot{\epsilon}_c$  increased linearly with applied stress; the correction for  $\dot{\epsilon}_\rho$  was negligible. Figure 7 shows the data for  $\dot{\epsilon}_c$  and  $\dot{\epsilon}_\rho$  vs relative density,  $\rho$ , at constant applied stress,  $\sigma_z$ . The curves have similar shapes, and the stresses are seen to cause large increases in the creep rate but only small increases in the densification rates, as observed earlier.<sup>14-17</sup>

The scanning electron micrographs of polished and etched surfaces of samples sintered for 5 min and 2 h are shown in Fig. 8(a) and (b). The grains are initially equiaxed but have a fairly wide distribution of sizes. During densification the grains grow and also become elongated. After sintering for 2 h at 915°C the average grain size is  $\approx 5 \mu\text{m}$  along the c-axis and  $\approx 2.5 \mu\text{m}$  perpendicular to the c-axis, giving an aspect ratio of about 2.

## 5. DISCUSSION

Previous work on other ceramic powders<sup>14-17</sup> has established that the ratio of the densification rate to the creep rate, i.e.  $\dot{\epsilon}_\rho/\dot{\epsilon}_c$ , is approximately constant during the intermediate stage of sintering, and that this ratio is specific to the system under investigation. It would be of interest to compare the data for the  $\text{YBa}_2\text{Cu}_3\text{O}_{6+\delta}$  system with those for other ceramic powders.

The volumetric densification rate,  $\dot{\epsilon}_\rho$ , and the creep strain rate,  $\dot{\epsilon}_c$ , may be expressed simply by the equations<sup>26</sup>

$$\dot{\epsilon}_\rho = (\Sigma/\phi + \sigma_z/3)/\eta_c \quad (8)$$

and

$$\dot{\epsilon}_c = \sigma_z / \eta_c \quad (9)$$

where  $\eta_\rho$  and  $\eta_c$  are the effective viscosities for densification and creep, respectively. Equations (8) and (9) give

$$\dot{\epsilon}_\rho / \dot{\epsilon}_c = (\eta_c / \eta_\rho) [(\Sigma / \phi) / \sigma_z + 1/3] \quad (10)$$

The ratio  $\dot{\epsilon}_\rho / \dot{\epsilon}_c$  can be found from the data of Fig. 7; the results are plotted in Fig. 9 together with those for a selection of materials studied earlier, i.e.  $\text{CdO}^{14}$  and  $\text{ZnO}^{15}$  (in which sintering occurs by solid state diffusion), a soda-lime glass<sup>16</sup> (viscous flow), and  $\text{MgO} + 5\text{w\% Bi}_2\text{O}_3^{17}$  (liquid phase). For  $\text{YBa}_2\text{Cu}_3\text{O}_{6+\delta}$  as well as the other materials indicated, this ratio is nearly constant over most of the intermediate stage of sintering. It is interesting to note that  $\dot{\epsilon}_\rho / \dot{\epsilon}_c$  for  $\text{YBa}_2\text{Cu}_3\text{O}_{6+\delta}$  falls between the data for the solid state sintering materials and the glass, but is very close to the data for the  $\text{MgO-Bi}_2\text{O}_3$  system that sinters by a liquid phase mechanism. The  $\dot{\epsilon}_\rho / \dot{\epsilon}_\rho$  data for  $\text{YBa}_2\text{Cu}_3\text{O}_{6+\delta}$  can be seen as evidence for densification in the presence of a liquid phase in this system.

The ratio of the creep viscosity to the densification viscosity,  $\eta_c / \eta_\rho$ , is basic to the understanding of the interaction between densification and shear deformation. Its measurement is, however, somewhat difficult since it requires the simultaneous measurement of creep and densification data on the same sample and to a high precision. In addition, the applied stresses should be sufficient to produce a measureable increase in the densification rates but low enough to prevent a change in

the sintering mechanism. The present data provide a good opportunity for evaluating  $\eta_c/\eta_\rho$ . The creep viscosity,  $\eta_c$ , at different values of  $\rho$  was calculated from linear plots of  $\dot{\epsilon}_c$  vs  $\sigma_z$ , (Eq. (9)). Because of the small increase in the densification rates for the stresses used in this work,  $\eta_\rho$  was estimated from the equation

$$\eta_\rho \approx (\sigma_z/3)[\dot{\epsilon}_\rho(\sigma_z = 140 \text{ kPa}) - \dot{\epsilon}_\rho(\sigma_z = 0)] \quad (11)$$

The data gave values for  $\eta_c/\eta_\rho$  of 0.7, 0.9 and 0.8 for  $\rho = 0.6$ , 0.7, and 0.8, respectively. Assuming an average value of  $\approx 0.8$  over this density range, the sintering stress,  $\Sigma/\phi$ , was calculated using Eq. (10) and found to be  $\approx 400$  kPa. The value of  $\eta_c/\eta_\rho \approx 0.8$  is about half the value obtained for the  $\text{MgO-Bi}_2\text{O}_3$ <sup>17</sup> system in which sintering occurs by a liquid phase mechanism, and is consistent with the low values predicted by Scherer<sup>27,28</sup> from an analysis of the effective moduli for shear and bulk deformation. From the present data it is evident that relatively small uniaxial stresses ( $\approx 1$  MPa) can produce extensive shear deformation in addition to small but measurable increases in the densification rates during sintering of  $\text{YBa}_2\text{Cu}_3\text{O}_{6+\delta}$  powder compacts in air.

## 6. CONCLUSIONS

This study which was performed to achieve a better understanding of the densification process in  $\text{YBa}_2\text{Cu}_3\text{O}_{6+\delta}$  powder compacts has, in addition, provided data for the measurement of a number of important creep and densification parameters. The data show many similarities with those for other ceramic systems studied earlier.

A temperature range of 920 - 940°C was found to be appropriate for achieving high densities by conventional, pressureless sintering in air. The highest densities of  $\approx 95\%$  of the theoretical was obtained by sintering for 2 h at 935°C.

Small uniaxial stresses ( $<150$  kPa) applied during sintering produced extensive creep deformation and a small but measurable increase in the densification rate. The measured ratio of the densification rate to the creep rate provided evidence for densification in the presence of a liquid phase.

The data allowed the measurement of the ratio of the creep viscosity to the densification viscosity, which was nearly constant at  $\approx 0.8$  in the density range 0.6-0.8, and the sintering stress, which was  $\approx 400$  kPa. These results show that extensive shear deformation and significant increases in the densification rates can be produced by the application of relatively low uniaxial stresses ( $\approx 1$  MPa) during the sintering of  $\text{YBa}_2\text{Cu}_3\text{O}_{6+\delta}$ .

Acknowledgement: This work was supported by the Division of Materials Sciences, Office of Basic Energy Sciences, U.S. Department of Energy, under Contract No. DE-AC03-76SF00098. This work was performed in the Lawrence Berkeley Laboratory when Prof. M.N. Rahaman was Visiting Staff Scientist in the Materials and Chemical Sciences Division.

## REFERENCES

1. J.G. Bednorz and K.A. Muller, "Possible High  $T_c$  Superconductivity in the Ba-La-Cu-O System," *Z. Phys.*, B64 189-193 (1986).
2. M.K. Wu, J.R. Ashburn, C.H. Thong, P.H. Hor, R.L. Meng, L. Gao, Z. Huang, Y.Q. Wang, and C.W. Chu, "Superconductivity at 93K in a New Mixed-Phase Y-Ba-Cu-O Compound System at Ambient Pressure," *Phys. Rev. Lett.*, 58 908-910 (1987).
3. P.H. Hor, L. Gao, R.L. Meng, Z.J. Huang, Y.Q. Wang, K. Forster, J. Vassiliou, C.W. Chu, M.K. Wu, J.R. Ashburn, and C.J. Thong, "High-Pressure Study of the New La-Ba-Cu-O Superconducting Compound System," *Phys. Rev. Lett.*, 58 911-912 (1987).
4. L.C. Bourne, M.L. Cohen, W.N. Creager, M.F. Crommie, A.M. Stacy, and A. Zettl, "Onset of Superconductivity in Y-Ba-Cu-O at 100K," *Phys. Lett.*, A120 494-496 (1987).
5. J.M. Tarascon, L.H. Green, W.R. McKinnon, and G.W. Hull, "Superconductivity at 90K in a Multiphase Oxide of Y-Ba-Cu," *Phys. Rev.*, B35 7115-7118 (1987).
6. R.J. Cava, B. Batlogg, R.B. Van Dover, D.W. Murphy, S. Sunshine, T. Siegrist, J.P. Remeiker, E.A. Rietman, S. Zahurak, and G.P. Espinosa, "Bulk Superconductivity at 91K in a Single-Phase Oxygen-Deficient Perovskite  $Ba_2YCu_3O_{9-\delta}$ ," *Phys. Rev. Lett.*, 58 1676-1679 (1987).
7. D.R. Clarke, "The Development of High  $T_c$  Superconductors: An Introduction," *Adv. Ceram. Mater.*, 3 [3B] 273-292 (1987).
8. C.N.R. Rao, P. Ganguly, A.K. Raychauduri, R.A. Mohan Ram, and K. Sreedhar, "Identification of the Phase Responsible for High Temperature Superconductivity in Y-Ba-Cu Oxides," *Nature*, 326 856-857 (1987).

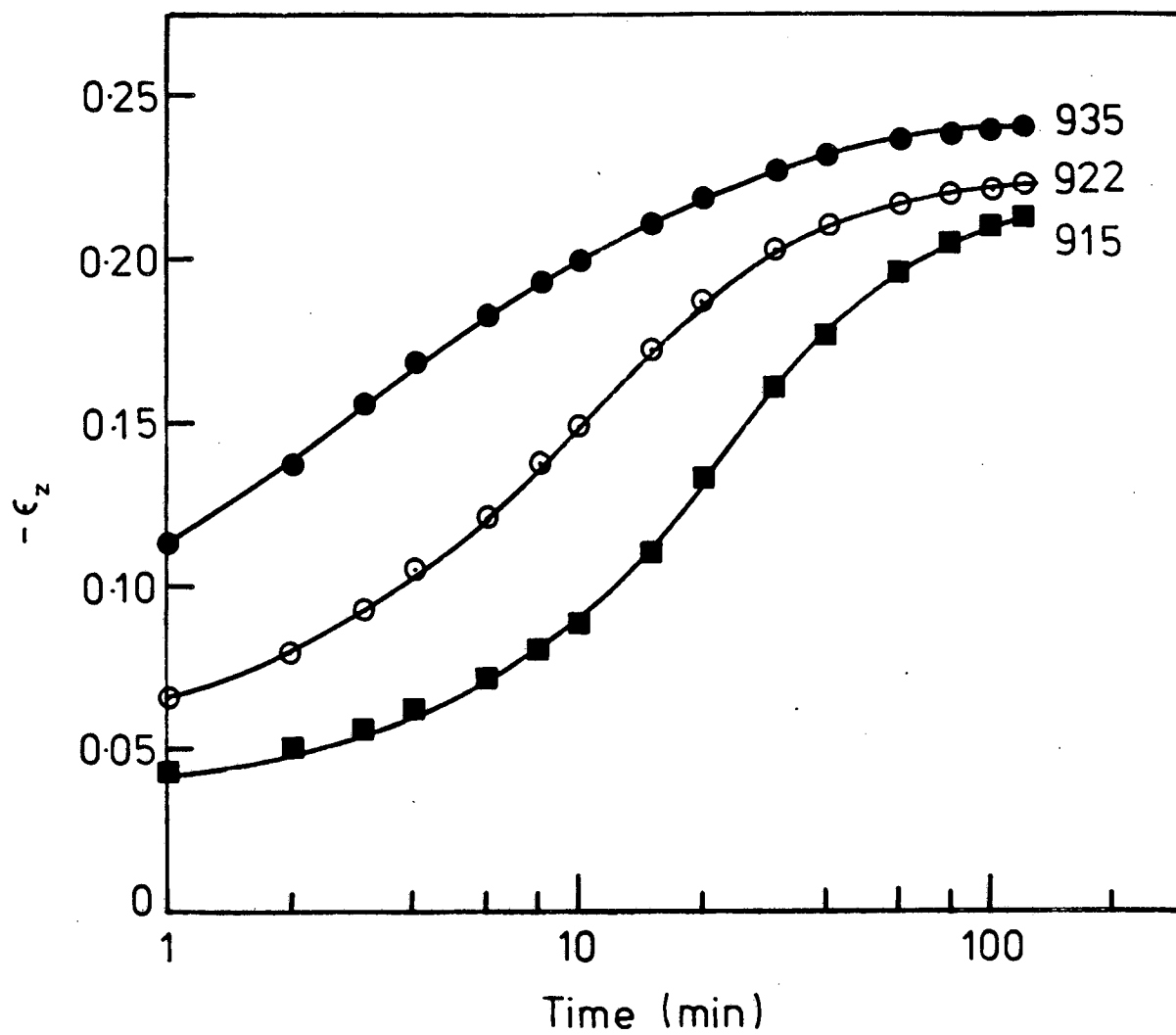
9. T. Siegrist, S. Sunshine, D.W. Murphy, R.J. Cava, and S.M. Zahurak, "Crystal Structure of the High  $T_c$  Superconductor  $Ba_2Y_1Cu_3O_{9-\delta}$ ," Phys. Rev., B35 7137-7139 (1987).
10. R.M. Hazan, L.W. Finger, R.J. Angel, C.T. Prewitt, N.L. Ross, H.K. Mao, and C.g.Hadidiacos, "Crystallographic Description of Phases in the Y-Ba-Cu-O Superconductor," Phys. Rev., B35 7238-7241 (1987).
11. P.M. Grant, R.B. Beyers, E.M. Engler, C. Lim, S.S.P. Parkin, M.L. Ramirez, V.Y. Lee, A. Nazzal, J.E. Vasquez, and R.J. Savoy, "Superconductivity Above 90K in the Compound  $YBa_2Cu_3O_x$ : Structural, Transport, and Magnetic Properties," Phys. Rev., B35 7242-7244 (1987)..
12. L.C. De Jonghe and M.N. Rahaman, "A Loading Dilatometer," Rev. Sci. Instrum., 55 [12] 2007-2010 (1984).
13. M.N. Rahaman and L.C. De Jonghe, "Sintering of CdO Under Low Applied Stress," J.Am. Ceram. Soc., 67 [10] C205-C207 (1984).
14. M.N. Rahaman, L.C. De Jonghe, and R.J. Brook, "Effect of Shear Stress on Sintering," J. Am. Ceram. Soc., 69 [1] 53-57 (1986).
15. M.N. Rahaman and L.C. De Jonghe, "Creep-Sintering of Zinc Oxide," J. Mater. Sci., (1987), in press.
16. M.N. Rahaman, L.C. De Jonghe, G.W. Scherer, and R. J. Brook, "Creep and Densification During Sintering of Glass Powder Compacts," J. Am. Ceram. Soc., 70 [10] 766-774 (1987).
17. L.C. De Jonghe and V. Srikanth, "Liquid Phase Sintering of  $MgO-Bi_2O_3$ ," submitted to J. Am. Ceram. Soc.
18. R. Raj, "Separation of Cavitation Strain and Creep Strain During Deformation," J. Am. Ceram. Soc., 65 [3] C46 (1982).
19. W. Beere, "A Unifying Theory of the Stability of Penetrating Liquid Phases and Sintering Pores," Acta Metall., 23 [1] 131-138 (1975).



## FIGURES

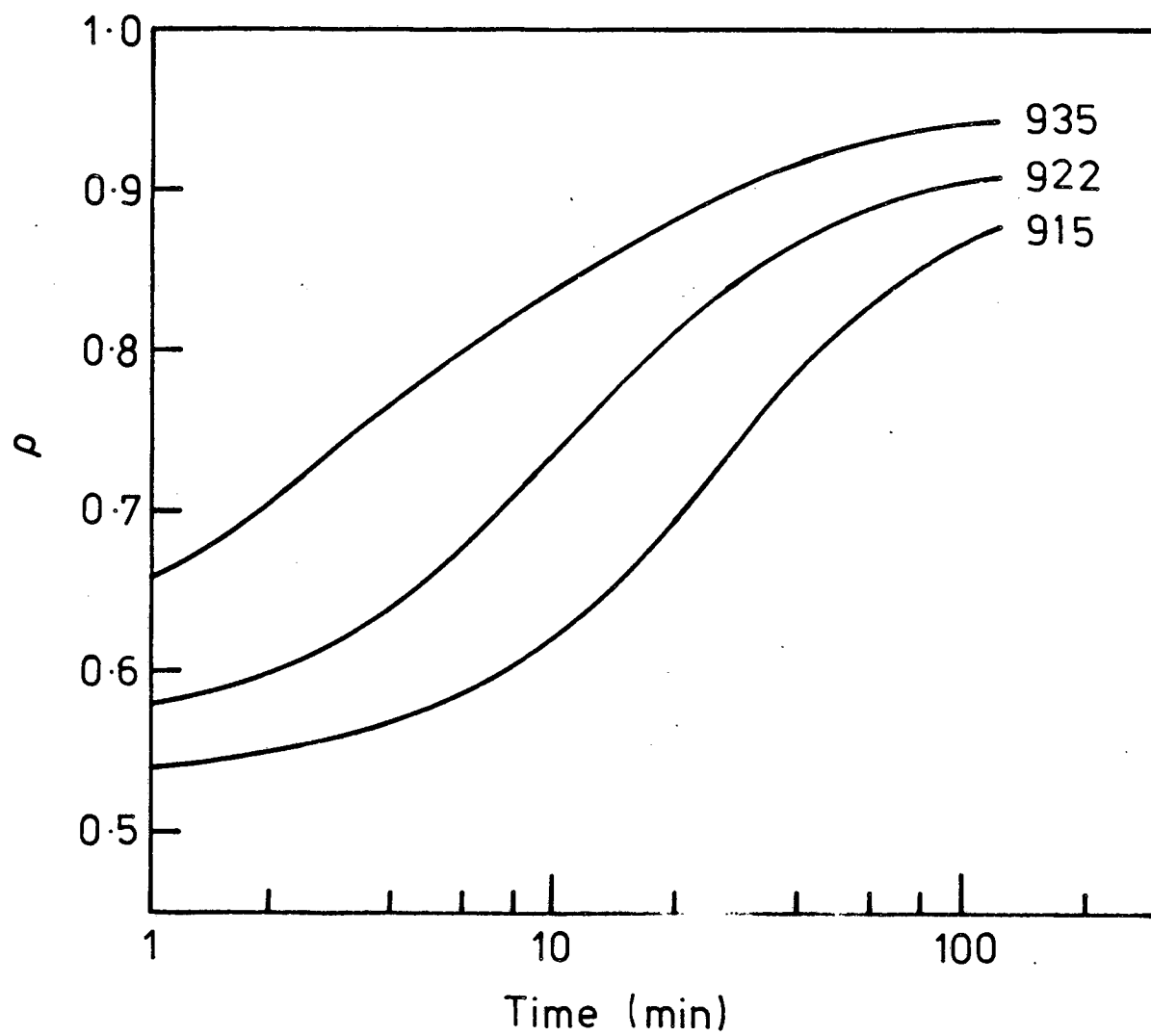
- FIG. 1. Axial strain vs time for  $\text{YBa}_2\text{Cu}_3\text{O}_{6+\delta}$  powder compacts sintered in air at the temperatures shown in °C.
- FIG. 2. Relative density vs time calculated from Fig. 1.
- FIG. 3. Axial strain vs time for  $\text{YBa}_2\text{Cu}_3\text{O}_{6+\delta}$  powder compacts sintered in air at 915°C under uniaxial stresses shown in kPa.
- FIG. 4. Axial strain vs radial strain for the experiments described in Fig. 3.
- FIG. 5. Creep strain vs time calculated from Figs. 3 and 4, and Eq. (3).
- FIG. 6. Relative density vs time calculated from Figs. 3 and 4, and Eq. (4).
- FIG. 7. Creep rate,  $\dot{\epsilon}_c$ , and densification rate,  $\dot{\epsilon}_\rho$ , vs relative density at constant uniaxial stresses shown in kPa.
- FIG. 8. Scanning electron micrographs of polished and etched surfaces of  $\text{YBa}_2\text{Cu}_3\text{O}_{6+\delta}$  powder compacts sintered in air at 915°C for (a) 5 min, and (b) 2 h. Bar = 4µm.
- FIG. 9. Ratio of the densification rate to the creep rate vs relative density for  $\text{YBa}_2\text{Cu}_3\text{O}_{6+\delta}$  compared with the data for other ceramic powders studied earlier. The data have been normalized at a constant uniaxial stress of 200 kPa.

20. W. Beere, "The Second Stage Sintering Kinetics of Powder Compacts," *Acta Metall.*, 23 [1] 139-145 (1975).
21. J.M. Vieira and R. J. Brook, "Kinetics of Hot-Pressing: The Semilogarithmic Law," *J. Am. Ceram. Soc.*, 67 [4] 245-249 (1984).
22. M.J. Cima and W.E. Rhine, "Powder Processing for Microstructural Control in Ceramic Superconductors," *Adv. Ceram. Mater.*, 2 [3B] 329-336 (1987).
23. C-T. Chu and B. Dunn, "Preparation of High- $T_c$  Superconducting Oxides by the Amorphous Citrate Process," *J. Am. Ceram. Soc.*, 70 [12] C375-C377 (1987).
24. S.M. Johnson, M.I. Gusman, D.J. Rowcliffe, T.H. Geballe, and J.Z. Sun, "Preparation of Superconducting Powders by Freeze-Drying," *Adv. Ceram. Mater.*, 2 [3B] 337-342 (1987).
25. A.C.D. Chaklader, G. Roemer, W.N. Hardy, J.H. Brewer, J.F. Carolan, and R.R. Parsons, "Studies on Ceramic Superconductors," *Adv. Ceram. Mater.*, 2 [3B] 556-561 (1987).
26. L.C. De Jonghe and M.N. Rahaman, "Sintering Stress of Homogeneous and Heterogeneous Powder Compacts," *Acta Metall.*, in press.
27. G.W. Scherer, "Sintering of Inhomogeneous Glasses: Application to Optical Waveguides," *J. Non-Cryst. Solids*, 34 239-256 (1979).
28. G.W. Scherer, "Sintering with Rigid Inclusions," *J. Am. Ceram. Soc.*, 70 [10] 719-725 (1987).



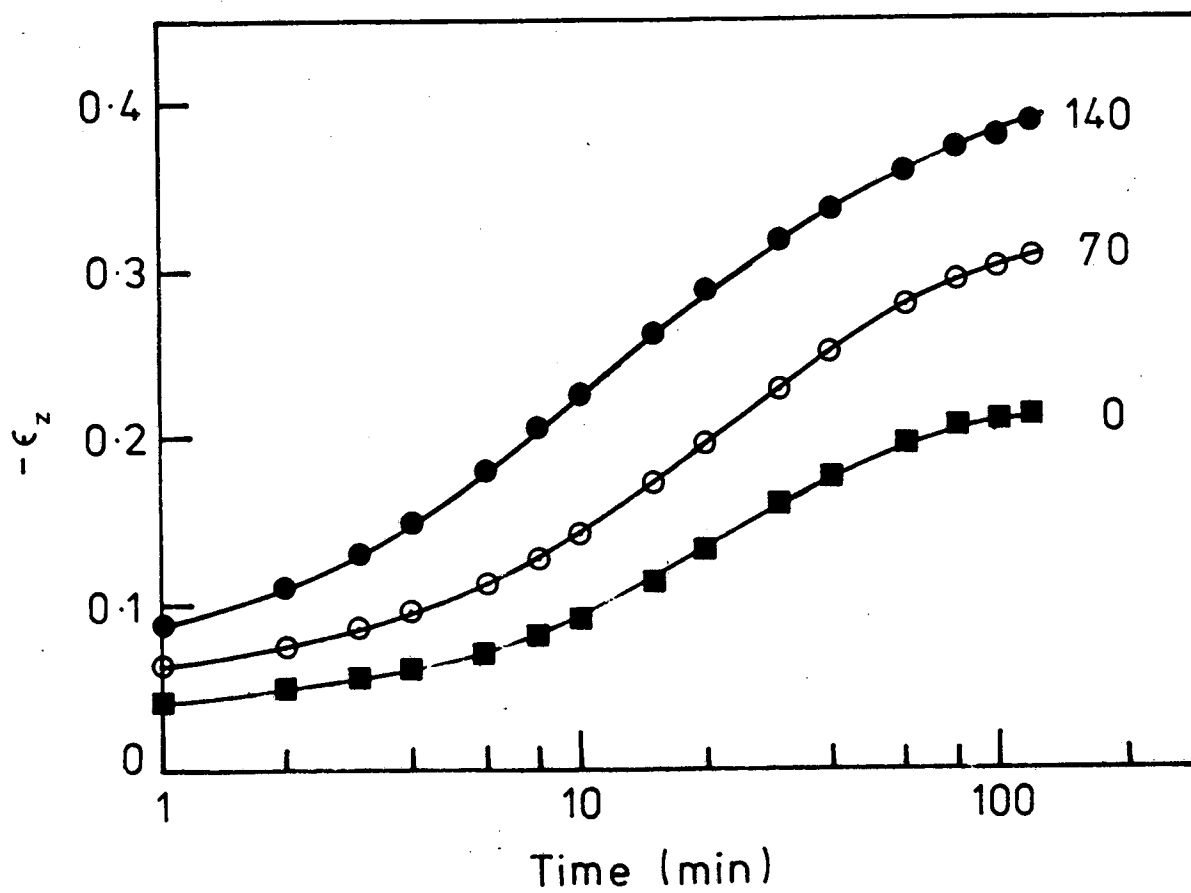
XBL 8712-5416

Fig. 1



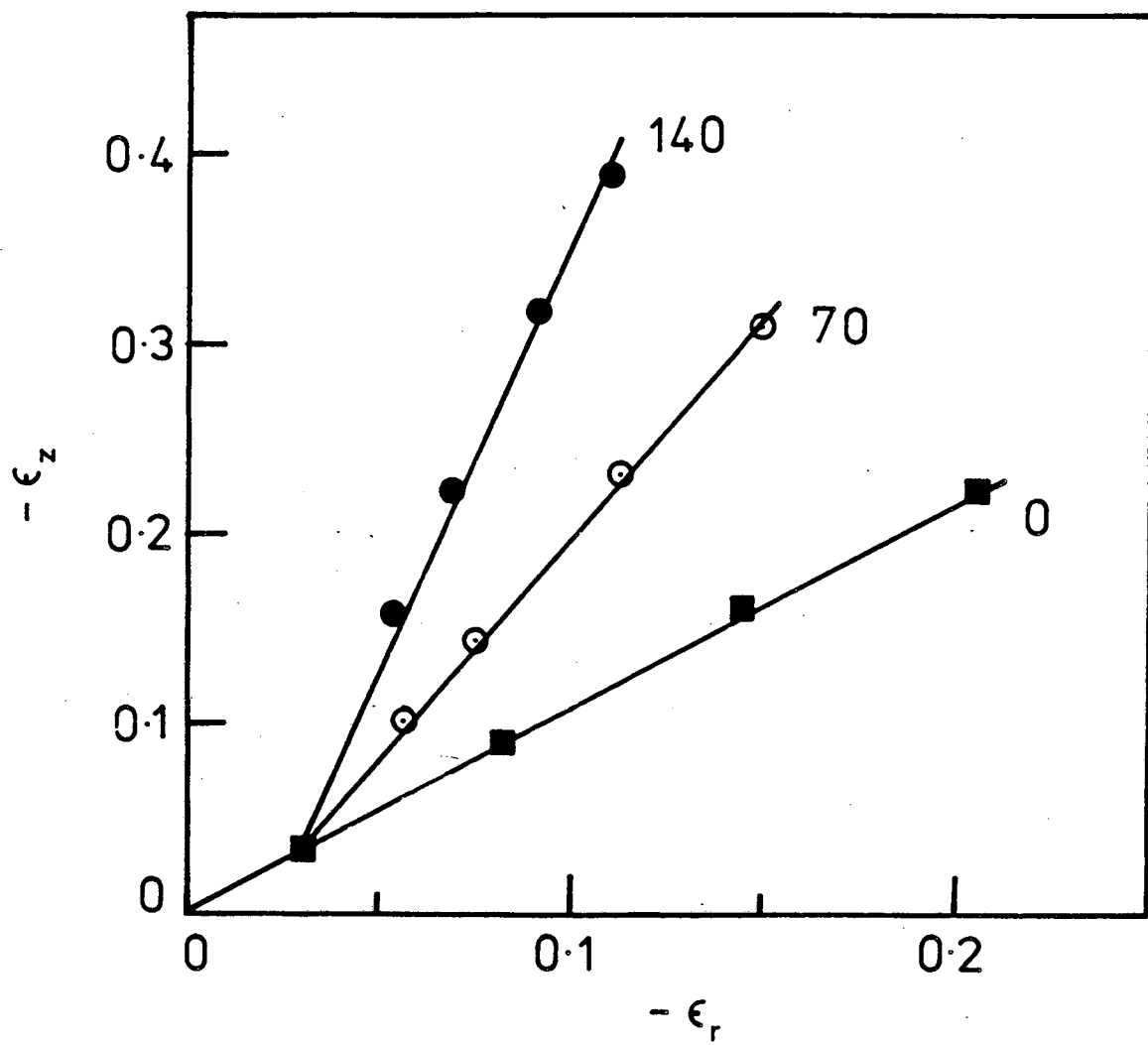
XBL 8712-5417

Fig. 2



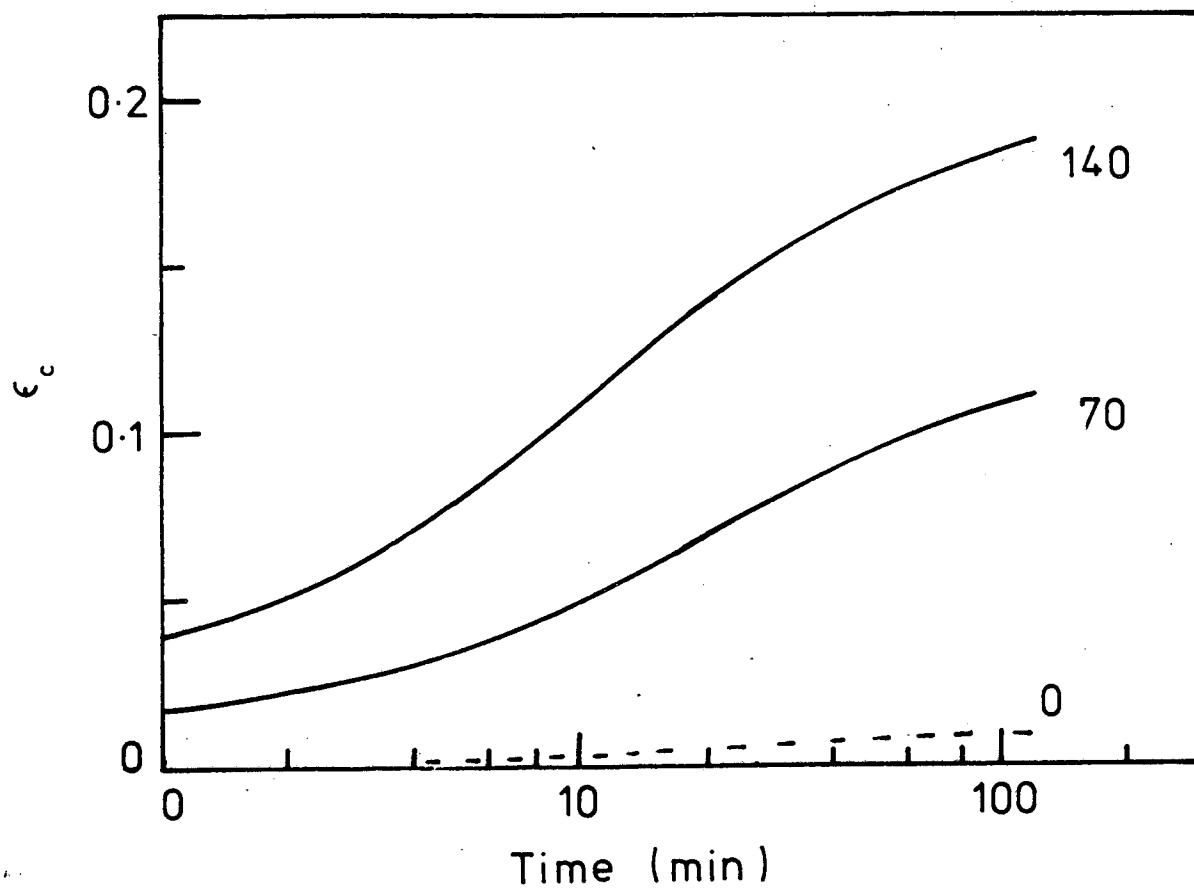
XBL 8712-5418

Fig. 3



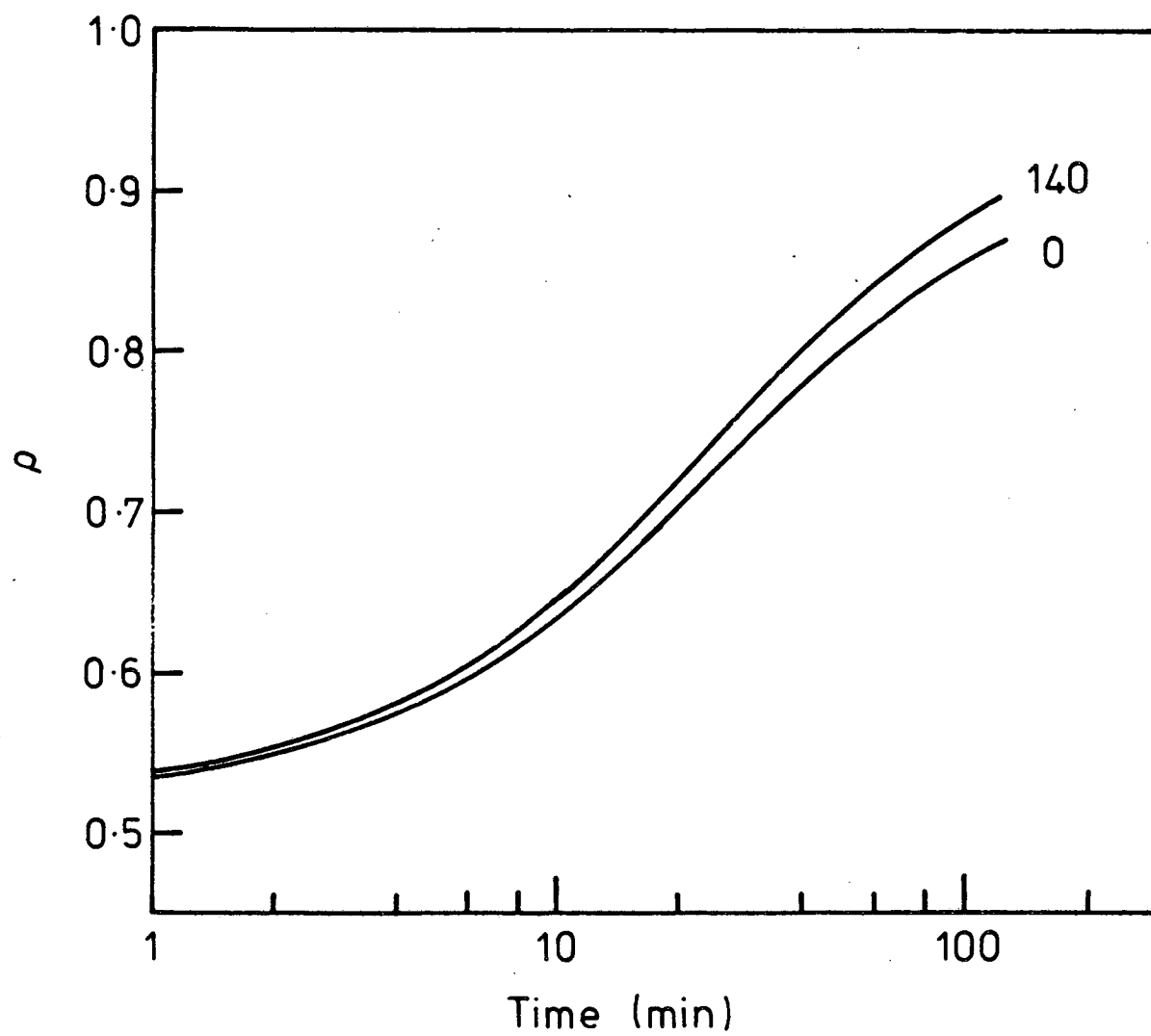
XBL 8712-5419

Fig. 4



XBL 8712-5420

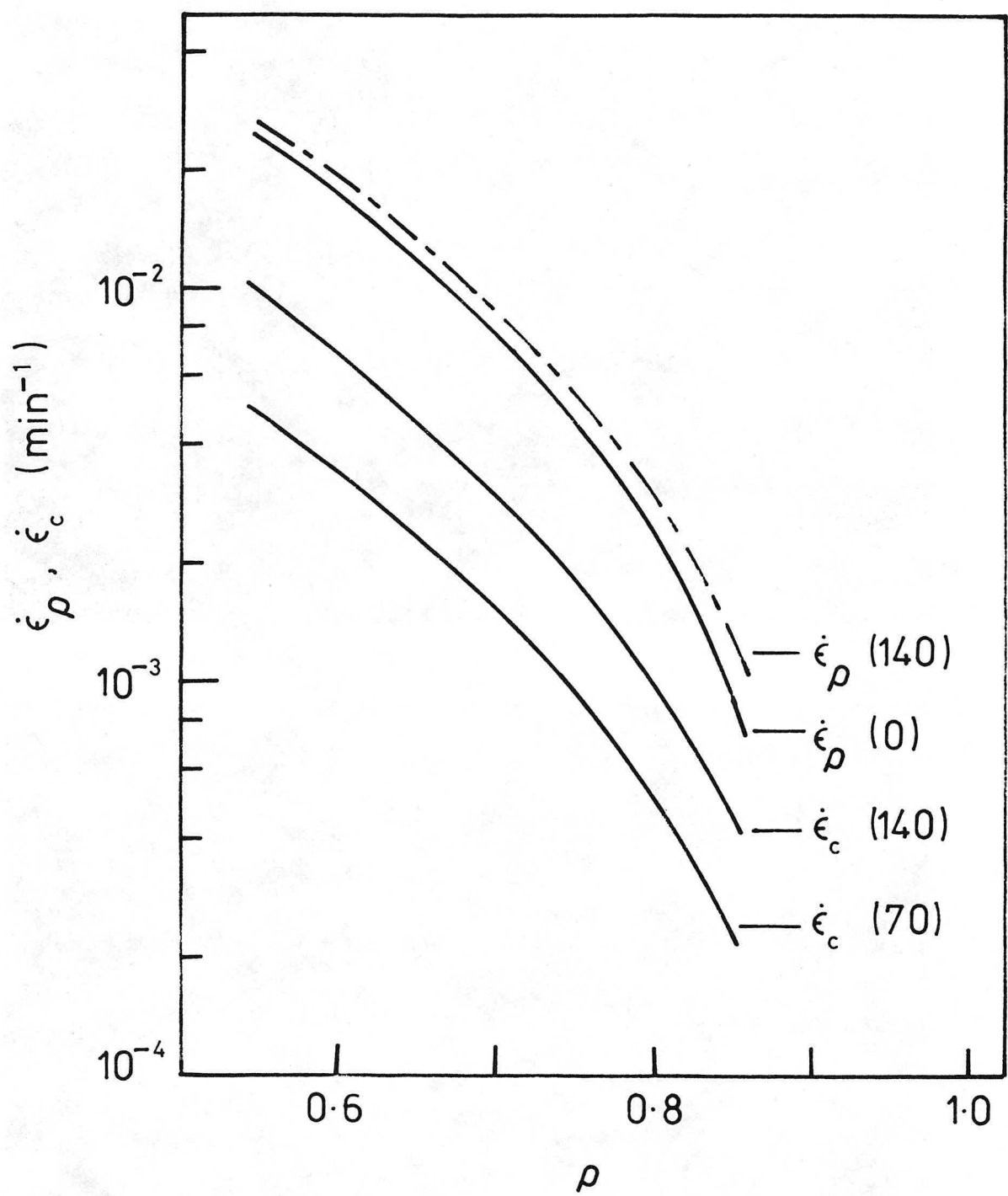
Fig. 5



XBL 8712-5421

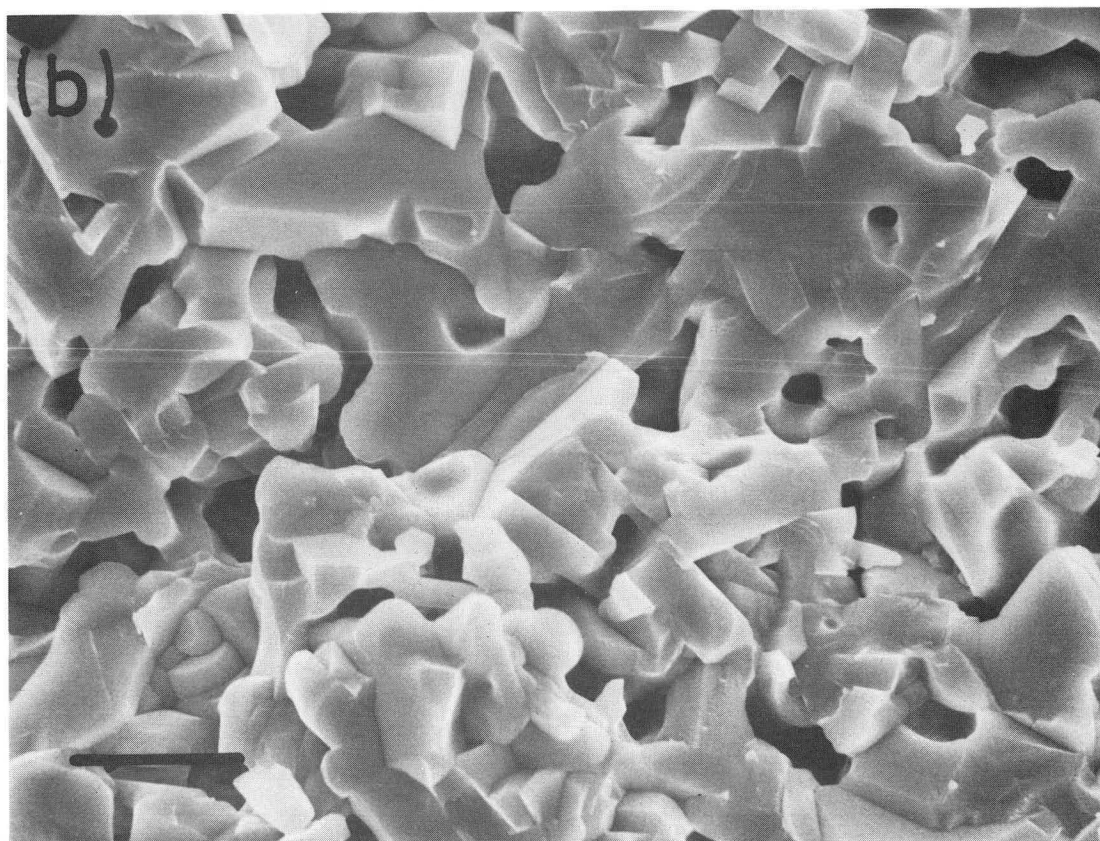
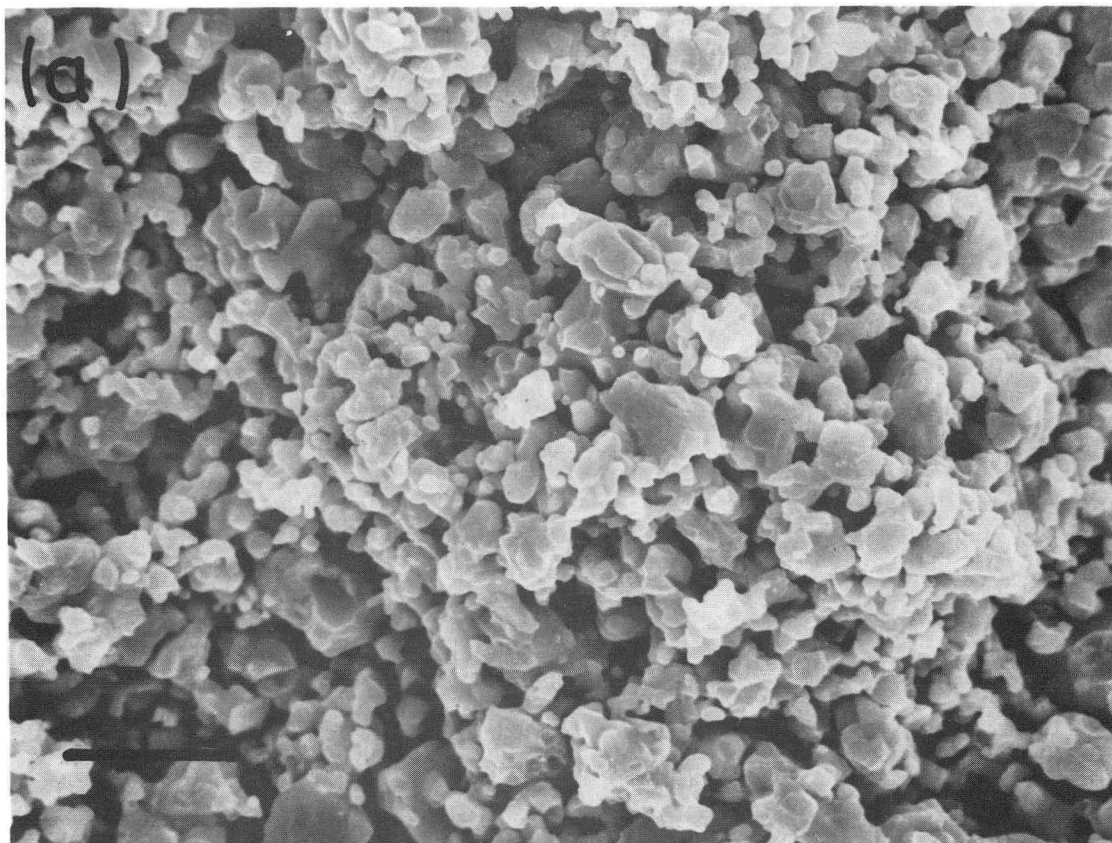
Fig. 6





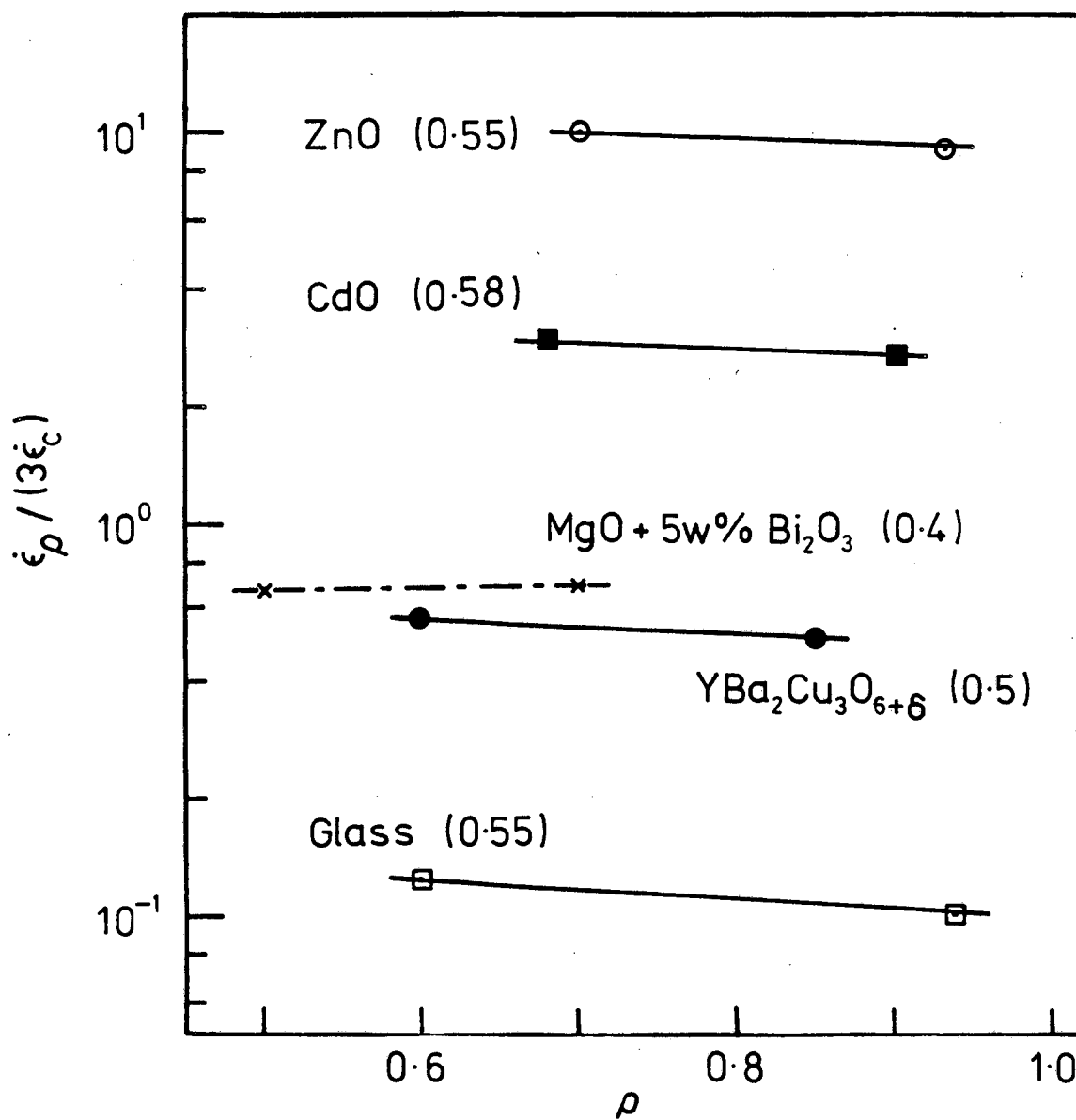
XBL 8712-5422

Fig. 7



XBB 870-1084

Fig. 8



XBL 8712-5423

Fig. 9

LAWRENCE BERKELEY LABORATORY  
TECHNICAL INFORMATION DEPARTMENT  
UNIVERSITY OF CALIFORNIA  
BERKELEY, CALIFORNIA 94720